RSC Advances

ROYAL SOCIETY OF CHEMISTRY

www.rsc.org/advances

Iron oxide nanoparticles immobilized PAN nanofibers: Synthesis and adsorption studies

Shabna Patel[a] & Garudadhwaj Hota[b*]
Department of Chemistry, NIT Rourkela, Orissa, India, 769008

Email:
[a] patel.shabna@gmail.com
[b] garud31@yahoo.com

***Corresponding Author**, Email: garud31@yahoo.com, garud@nitrkl.ac.in
Ph: 91-661-2462655 (O), Fax: 91-661-2462651

ABSTRACT

In this study we have prepared (Polyacrylonitrile) PAN/iron oxide composite nanofibers by three different methods and have compared their removal efficiency for the adsorption of Congo red (CR) dye from aqueous solution. In the first method, we have prepared electrospun PAN/iron(III) acetylacetonate composite nanofibers by electrospinning followed by hydrothermal method for in situ growth of iron oxide nanoparticles on the surface of PAN nanofibers. In the second method the electrospun PAN nanofibers were immersed into the iron alkoxide solution followed by hydrolysis reaction at 80^0C. In the third method, PAN/iron oxide composite nanofibers were prepared by blending the previously prepared iron oxide nanoparticles with PAN solution followed by electrospinning technique. The obtained different nanocomposite fibers were characterized by Attenuated Total Reflectance-Fourier Transform Infrared (ATR- FTIR), X-ray diffraction (XRD), and Field Emission Scanning Electron Microscopy (FE-SEM) analytical techniques. FE-SEM images clearly show the formation of iron oxide nanoparticles that are uniformly decorated on the surface of PAN nanofibers after hydrothermal reactions. The average diameters of the nanoparticles are observed to be in the range of 30 to 120 nm. The adsorption experiments such as effect of pH, contact time, initial concentration variation, and temperature were explored in the batch experiments. CR dye is used as a model organic pollutant for adsorption study. The adsorption isotherm, kinetic study and thermodynamic study were also carried out to elucidate the adsorption mechanism.

KEYWORDS: Electrospinning, Iron oxide, Nanocomposite fibers, Adsorption, Congo red

1. Introduction

Nowadays number of dyes is being widely used in many manufacturing industries such as textile, paper, rubber, plastic, cosmetic, pharmaceutical, and food, which generate huge volume of waste water containing large amount of dissolved dyestuffs and other toxic products.[1] The discharge of these dyes effluents in the environment is a serious matter of concern for both toxicological and aesthetical reasons.[2] Among these dyes, CR (an anionic dye) has many toxic and carcinogenic effects on both human and other living organisms. CR [1-naphthalene sulphonic acid, 3,30-(4,40-biphenylenebis (azo)) bis (4-amino-) disodium salt, CR] has been known to cause allergic reaction and metabolized to benzidine, which is carcinogenic to human beings.[2,3] Therefore, treatment of waste water containing these dyestuffs has been hot spot of current research. Various physical, chemical and biological methods like adsorption, biosorption, chemical oxidation, electrochemical reduction, membrane separation, biodegradation, photo-degradation have been widely applied for treatment of dye-bearing effluent.[4-6] However, adsorption is one of the most promising methods for removal of dyestuffs from waste water due to its low cost, high efficiency and easy operation.[7]

In contrast to bulk materials, nanostructured adsorbents draw more attention, because of their higher surface-to-volume ratio, larger specific surface area, and uniform pore size distribution. Recently, Mahapatra et al., have reported the removal of CR dye from aqueous solution using mixed iron oxide-alumina nanocomposite adsorbent.[8] However; there are some issues, which restrict the practical applications of these nanostructured adsorbents, especially nanoparticles. Due to the high surface energy, small size nano range and powdered morphology, it is difficult to separate them from the liquid phase after use.[9,10] Recent scientific and technological interest has focused on polymer-inorganic nanocomposite membrane, where inorganic nanoparticles are immobilized into the polymer membrane. The

incorporation of inorganic nanoparticle into the polymer matrix will significantly enhance the mechanical, thermal, chemical stability and working performance of the nanocomposite membrane in the field of energy, environment and biomedical.[11,12] In recent years, electrospinning has been widely used as an effective and facile approach for the fabrication of polymer-inorganic nanocomposite fibers. By the electrospinning process, various nanomaterials can be introduced into the polymer matrix in order to enhance the physical, chemical and catalytic properties of the polymer fibers.[13] Polyacrylonitrile (PAN) has been used to produce nanofibers due to its excellent characteristics such as commercial availability, desirable chemical resistance, thermal stability, good mechanical properties, vast possibilities for surface functionalization as well as non-toxic in nature.[14,15] Recently, Kim et al., have reported electrospun ZnO- nylon 6 nanocomposite fibers for photo-degradation of Methylene blue (MB) dye.[11] However, among the inorganic materials, iron oxide materials are widely used in removal of heavy metal ions and organic pollutants due to their low cost, extensive availability, reactive surface, chemical stability and high efficiency. More recently, Khosravi et al. synthesized magnetic iron oxide nanospheres for removal of anionic dyes such as reactive orange and reactive yellow from aqueous solution.[16] Li et al. have reported the fabrication of nylon 6/iron oxide composite nanofibrous membrane by electrospinning and their application for the removal of Cr (VI) ions form the aqueous phase.[10]

In the present study, we have prepared PAN/iron oxide nanocomposite fibers by three different methods and then compared their removal efficiency for the adsorption of CR dye from aqueous solution. First, PAN/iron(III) acetylacetonate homogeneous solution were electrospun into composite nanofibers followed by hydrothermal treatment for in situ growth of iron oxide nanoparticles on the surface of PAN nanofibers. Second, electrospun PAN/iron oxide nanocomposite fibers were prepared by blending the previously prepared iron oxide nanoparticles with PAN solution followed by electrospinning technique. In the third method,

in order to grow iron oxide nanoparticles on the surface of PAN nanofibers, the e-spun PAN nanofibers were immersed into iron alkoxide solution followed by hydrothermal reaction at 80° C. The adsorption experiments such as effect of pH, contact time, initial concentration, and temperature were explored in the batch experiments. The adsorption isotherm, kinetic study and thermodynamic study were also carried out to elucidate the adsorption mechanism.

2. Materials and Methods

2.1. Materials

The polymer polyacrylonitrile (PAN; Mw = 1, 50,000) and Iron (III) acetylacetonate were purchased from Sigma Aldrich (USA). N, N-Dimethylformamide (DMF), Ethylenediamine, Sodium Hydroxide (NaOH), Hydrochloric acid (HCl), Congo red (CR) dye, Iron(II) chloride tetrahydrate ($FeCl_2$. $4H_2O$), Ammonia solution and ethanol were purchased from Merck (INDIA). Ethylene Glycol (EG) was purchased from NICE Laboratory reagents (INDIA). Double distilled water was used in throughout the experiments. All the chemicals were used without further purifications.

2.2. Synthesis of Electrospun PAN/Iron acetylacetonate Nanofiber Membrane

8 wt % PAN solution was prepared by dissolving PAN polymer powder in DMF, taken as solvent. Then mechanical stirring was applied for 12 hours in order to obtain a homogeneous clear solution of PAN. To the resulting PAN solution, iron (III) acetylacetonate was added and polymer to iron precursor ratio was kept at 3:2. Then mechanical stirring was applied for 12 hours to obtain the homogeneous PAN/iron (III) acetylacetonate electrospinning solution, which was loaded into a 5 mL plastic syringe fitted with a metallic needle. Then by using syringe pump the electrospinning solution was pushed to the needle tip with a flow rate of 1 mL/h. The distance was set to 12 cm between needle tip and the grounded metal collector covered with a sheet of aluminium foil, which was served as counter electrode. A positive charge high voltage of 13 kV was applied to the needle tip by using high voltage power

supply (Glassman, Japan). The electrospinning process was carried out at room temperature with a relatively low humidity (45- 50%) condition.

2.2.1. In Situ Hydrothermal Growth of Iron Oxide Nanoparticles on PAN Nanofibers

The obtained PAN/Iron(III) acetylacetonate composite nanofibers membrane was firstly put into glass beaker containing 70 mL deionised water and then the pH of the water was maintained at 10-11 using ethylene diamine. After that the deionised water with nanofibers membrane was transferred into 100 mL Teflon lined autoclave for hydrothermal reaction. The hydrothermal process was conducted at 150°C for 12 hours. After reaction, the PAN/iron oxide composite nanofibers membrane was removed, washed with distilled water and then dried in electric oven at the temperature of 60°C.

2.3. Preparation of Iron Oxide Nanoparticles by Hydrothermal Process

The iron oxide nanoaparticles were synthesized by hydrothermal method. In this method, iron (III) acetylacetonate was dissolved in 70 mL deionised water taken in a beaker. Then ethylenediamine was added drop wise into the solution under stirring condition to maintain the pH at 10-11. After that the resulting suspension was transferred into the 100 mL Teflon lined autoclave and the hydrothermal reaction was carried out at 150°C for 12 hours. After the reaction, the precipitate obtained was centrifuged, washed with distilled water repeatedly and finally with alcohol. Then the obtained precipitate was dried in electric oven at 60°C.

2.3.1. Synthesis of Electrospun PAN/Iron Oxide Nanocomposite Fibers

The obtained iron oxide nanoparticles were mixed into the previously prepared 8 wt% PAN solution and the polymer to particle ratio was maintained at 3:2. Then the resultant colloid solution was kept under stirring for 2 hours to make the fine dispersion of iron oxide nanoparticles. After that, the iron oxide nanoparticles blended PAN solution was electrospun at an applied voltage of about 13 kV and with a flow rate of 1 mL/h to form PAN/iron oxide composite nanofibers.

2.4. Synthesis of PAN/IA Nanofibers

We have also prepared electrospun PAN nanofibers membrane by using 8 wt % PAN-DMF solution and was maintained the similar electrospinning condition as earlier. Then the PAN/IA nanofibers membrane was prepared via complexation of espun PAN nanofibers with iron(II) salt in presence of EG. In a typical procedure, 0.5g of $FeCl_2$ $4H_2O$ was dissolved into 10 mL of EG, which coordinated with $FeCl_2$. $4H_2O$ to form iron alkoxide (IA). As a result, HCl was formed in the solution as a by-product, which inhibits the further formation of IA. Then 0.5 mL of ammonia solution was added into the solution to neutralize HCl and the colour of the solution turned dark green. After that, the previously prepared electrospun PAN nanofibers membrane was immersed into the IA solution for 2 h, during which the functional groups (-C≡N) of PAN will form co-ordination bonds with Fe(II) on the surface of PAN nanofibers, resulting PAN/IA nanofibers membrane.

2.4.1. Growth of Iron Oxide Nanoparticles on the Surface of PAN nanofibers

The obtained PAN/IA nanofibers membrane was immersed into a glass beaker containing 100 mL of deionised water placed in electric heated thermostatic water bath at the temperature of 80°C for 1 h in order to conduct the hydrothermal reaction. After the hydrolysis reaction, the PAN/iron oxide nanocomposite fibers membrane was removed from the water and dried in an electric oven at 60°C.

The schematic representation for the synthesis of PAN/iron oxide composite nanofibers membrane is shown in figure 1.

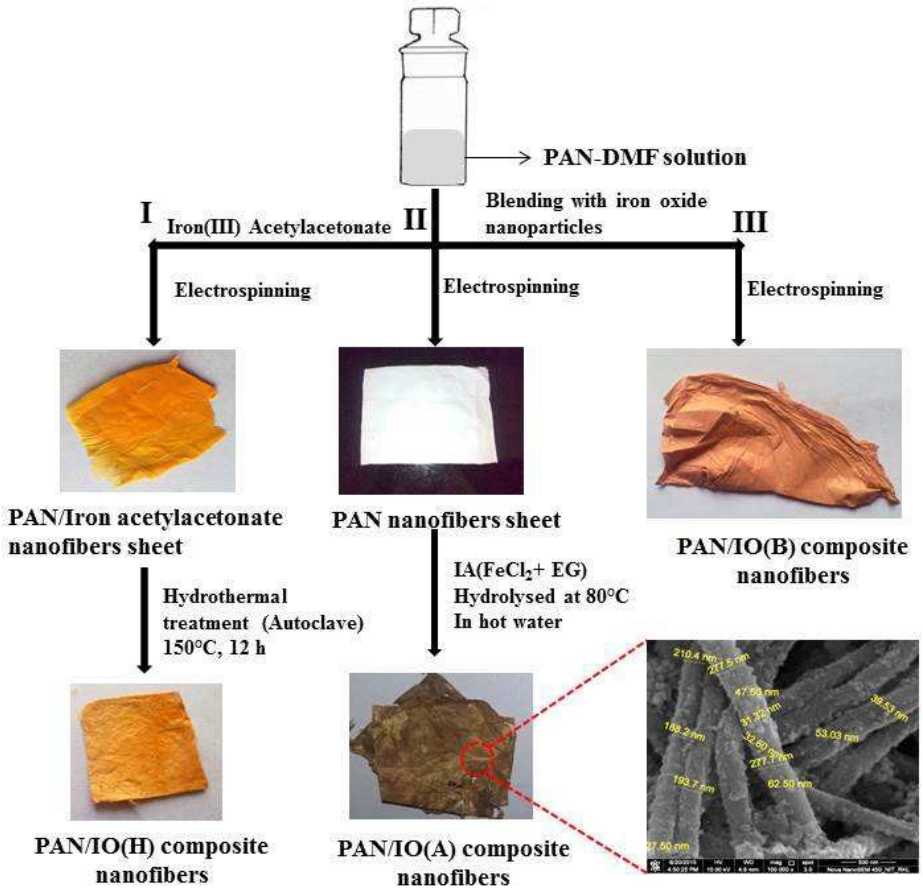

Figure 1: Schematic representation for different synthetic methods of PAN/iron oxide composite nanofibers membranes

In order to make clear identification of the PAN/iron oxide composite nanofibers membrane, we have used the following three different notations. The iron oxide nanoparticles which are hydrothermally grown on the surface of PAN nanofibers is named as PAN/IO(H) composite nanofibers, whereas PAN/iron oxide composite membrane, in which iron oxide nanoparticles are blended into the PAN nanofibers matrix is named as PAN/IO(B). The PAN/iron oxide composite nanofibers where e-spun PAN membrane was immersed into alkoxide solution followed by hydrothermal reaction is named as PAN/IO(A) composite nanofibers.

2.5. Characterization Techniques

The functional groups of the prepared composite nanofibers membranes were characterized by attenuated total reflectance-fourier transform infrared spectrometry (ATR-FTIR) on a Nicolet IR100 Spectrometer in the range of wave number from 4000-400 cm^{-1}. The structural characterization was carried out by X-ray diffraction (XRD) in a Rigaku X-ray diffractometer operated with Cu Kα radiation (λ = 1.540 Å). The surface morphology of the nanofibers membranes were examined using field emission scanning electron microscope (FE-SEM) (NOVA NANO SEM_450). Carl-Zeiss FESEM (Carl-Zeiss Supra 55) equipped with Oxford INCA energy dispersive X-ray analyser system for elemental composition of composite nanofibers membrane. A digital pH meter (Sartorius Mechatronics India Pvt. Ltd), fitted with a glass electrode was used for pH adjustment of desired value. In the adsorption experiment, the residual concentration of CR dye solution was measured using Shimadzu 2450 Spectrophotometer. The iron leaching experiment was performed by using Perkin Elmer optima 7000 DV ICP-OES spectrometer.

2.6. Adsorption Experiment for CR Dye by Batch Process

The PAN/IO(H), PAN/IO(B) and PAN/IO(A) nanocomposite fibers membrane were used as adsorbent for the removal of CR dye from aqueous system. A stock solution of 1000 mg/L was prepared by dissolving proper amount of CR dye in deionised water. Solutions with required concentrations of CR dye were prepared by successive dilutions of stock solution. Batch adsorption experiments were conducted in order to investigate the effects of solution pH (3-10), contact time (15-180 min), initial CR dye concentration (20-70 mg/L) and temperature (303 K, 313 K and 323 K) for adsorption of CR dye onto the PAN/iron oxide composite nanofibers surface. In the adsorption experiment, the adsorbent dosage was 0.03g and the volume of CR dye solution was 20 mL. After the batch adsorption experiment, the

residual concentrations of the CR dye in the aliquot were detected using UV-Visible spectrophotometer by measuring the absorbance of the solution at λ_{max} = 498 nm. All the batch adsorption experiments were carried out at room temperature.

3. Results and Discussion

3.1 Structural Characterization

3.1.1. ATR-FTIR Analysis

The bonding configurations of the resultant PAN/IO composite nanofibers were performed by using ATR-FTIR spectroscopy. Figure 2 shows the ATR-FTIR spectra of electrospun PAN nanofibers and PAN/IO composite nanofibers. For the electrospun PAN nanofibers (figure 2(a)), the prominent peaks at 2240, 2932, and 1450 cm^{-1} are due to the stretching vibrations of nitrile groups (C≡N), stretching and bending vibrations of methylene groups (-CH_2-), respectively. The FTIR spectrum of pristine PAN nanofibers also contains prominent peaks at 3604 and 1730 cm^{-1}, which may be attributed to the stretching vibrations of the (N-H) and carbonyl groups, respectively for residual solvent DMF; as it has been used as solvent during electrospinning process.[14,15] However, for the PAN/IO(H), PAN/IO(B) and PAN/IO(A) composite nanofibers, a new absorption peak has appeared at 575 cm^{-1} assigned to the (Fe-O) stretching vibrations of iron oxide nanoparticles. The enhanced intensity for (Fe-O) is indicative of high iron loading in the PAN/IO composite nanofibers.[17]

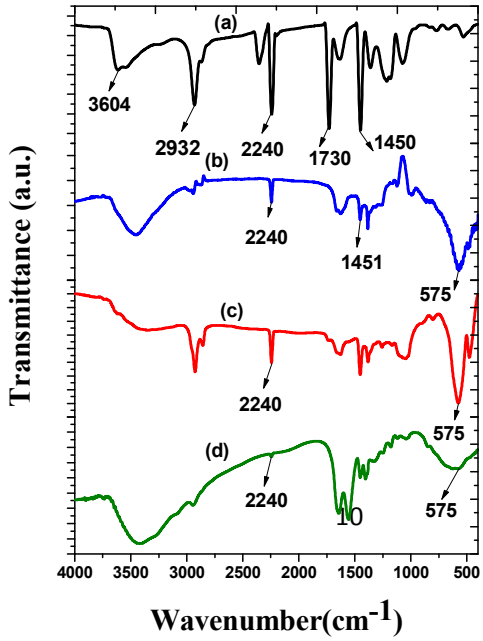

Figure 2: ATR-FTIR spectra of (a) PAN nanofibers, (b) PAN/IO(H), (c) PAN/IO(B) and (d) PAN/IO(A) composite nanofibers

3.1.2. X-Ray Diffraction Analysis

XRD is used to investigate the phase structure of the pristine PAN and PAN/IO composite nanofibers and the results obtained were shown in figure 3. From figure 3(a) it can be observed that, the XRD pattern of pristine PAN nanofibers shows a sharp crystalline peak at a diffraction angle of 2θ of 17° due to the hexagonal packing of rod like chains and the amorphous nature of the sample.[15,18] In case of XRD pattern of both the composite nanofibers (figure 3(b) and (c)), the intense diffraction peaks at 24.3°, 32.43°, 35.88°, 41.06°, 49.67° and 54.25° are corresponding to the (012), (104), (110), (113), (024) and (116) planes of hematite (α-Fe_2O_3), which is consistent with the JCPDS data (JCPDS- 24-0072). However, the intensity of the diffraction peaks for PAN nanofibers has been decreased in case of both the composite nanofibers due to the incorporation of iron oxide nanoparticles. In the XRD pattern of PAN/IO(A) composite nanofibers (figure 3(d)) , the diffraction peaks at 30.04°, 35.63°, 43.38°, 57.13°, and 62.89° correspond to the (220), (311), 400), (511), and (440) planes, which is ascribed to maghemite (γ- Fe_2O_3) phase with JCPDS data (JCPDS-39-1346).

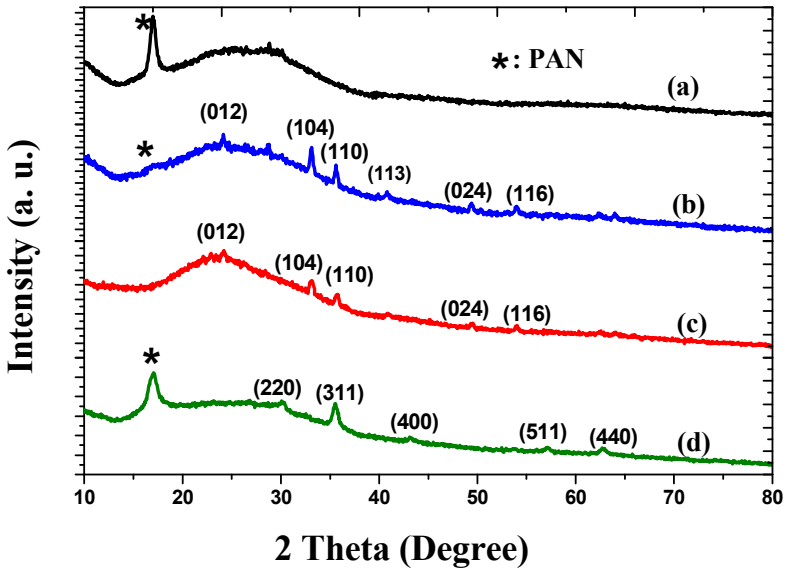

Figure 3: XRD pattern of (a) PAN nanofibers, (b) PAN/IO(B), (c) PAN/IO(H) and (d) PAN/IO(A) composite nanofibers

3.1.3. SEM-EDAX Analysis

In order to characterize the surface morphology and fiber dimension, we have carried out the FE-SEM studies of PAN/iron oxide composite nanofibers. Figure 4 represents the FE-SEM images and EDAX spectrum of PAN/IO(H) composite nanofibers. From figure 4(a) and (b) it can be seen that after hydrothermal treatment, the iron oxide nanoparticles are uniformly decorated on the surface of the PAN nanofibers. The diameters of the iron oxide nanoparticles are observed to be in the range of 80 to 120 nm. However, the diameters of the composite fibers are found to be in the range of 450 to 650 nm. The EDAX data shows the presence of iron and oxygen elements in the composite nanofibers (Fig 4c) and weight percentage of iron is found to be 22 % in this case. The FE-SEM images and EDAX spectrum of PAN/IO(B) composite nanofibers are shown in figure 5. From figure 5(a) and (b), it can be observed that the nanocomposite fibers are randomly arranged and exhibits smooth surface. However, some nodes like structures are present in the composite nanofibers due to the blending of iron oxide nanoparticles in the PAN polymer solution. The EDAX spectra of composite nanofibers (figure 5c) confirm the incorporation of iron oxide nanoparticles in the PAN nanofibers matrix. The weight percentage of iron is found to be 8% in case of PAN/IO(B) composite nanofibers.

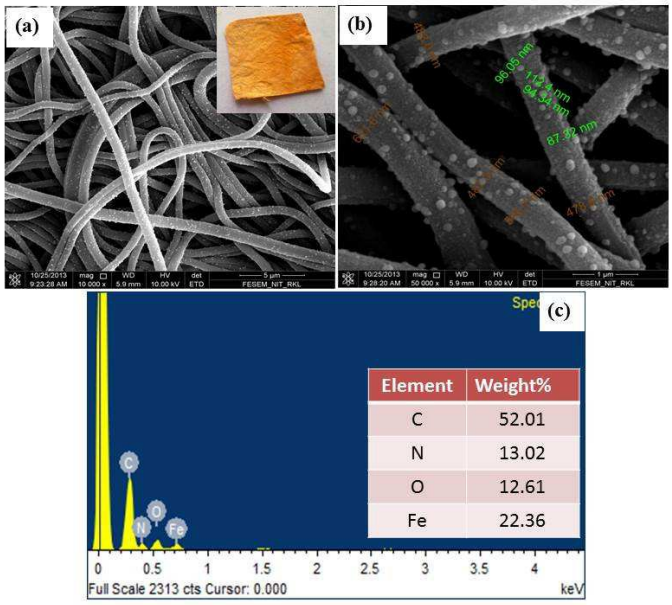

Figure 4: Low and high magnification FE-SEM images (a, b), and EDAX spectrum (c) of PAN/IO(H) composite nanofibers (inset: photograph)

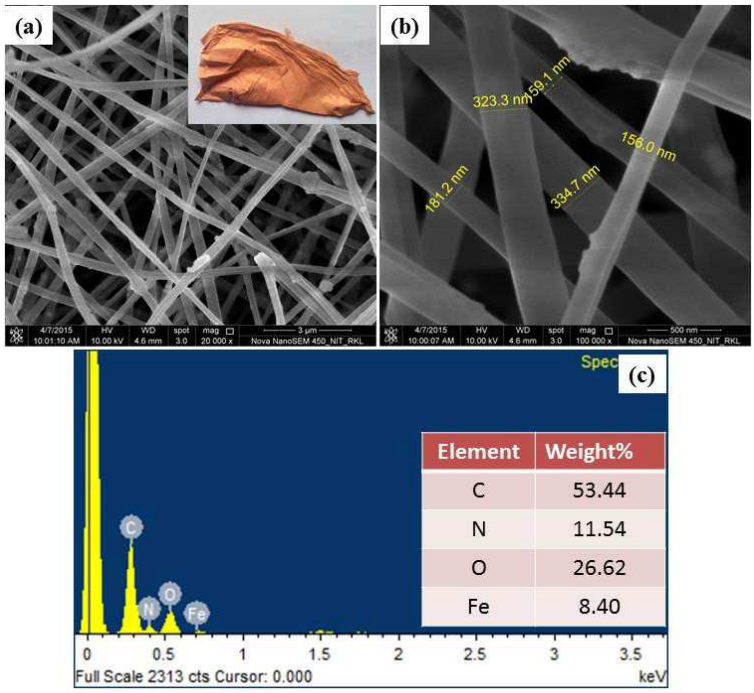

Figure 5: Low and high magnification FE-SEM images (a, b), and EDAX spectrum (c) of PAN/IO(B) composite nanofibers (inset: photograph)

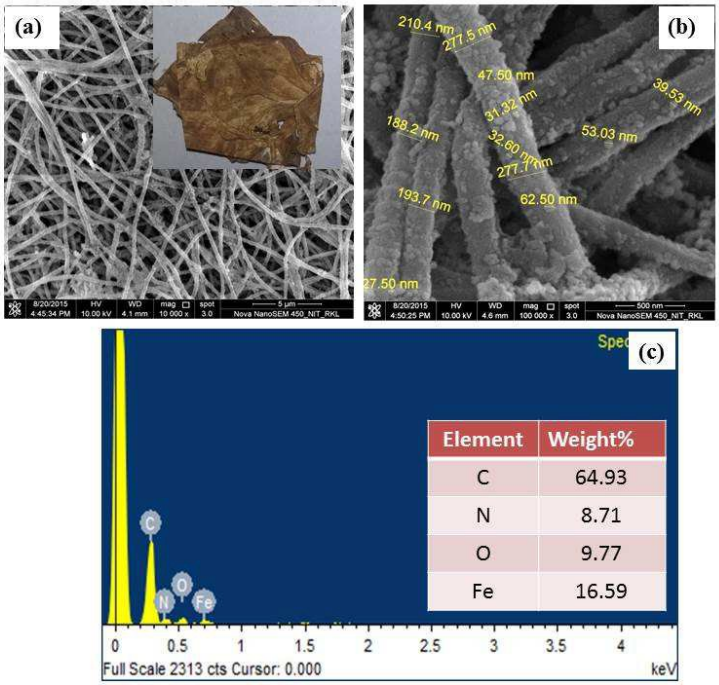

Figure 6: Low and high magnification FE-SEM images (a, b), and EDAX spectrum (c) of PAN/IO(A) composite nanofibers (inset: photograph)

Figure 6 represents the FE-SEM images of PAN/IO(A) composite nanofibers. From figure 6(a) and (b), it is observed that the nano-sized iron oxide particles are impregnated with the surface of PAN nanofibers and the average diameter of the nanoparticles are found to be in the range of 30 to 70 nm. The EDAX study clearly suggest the presence of iron oxide in the PAN/IO(A) composite nanofibers (Figure 6c). It is also observed from the EDAX studies that the weight percentages of iron in case of PAN/IO (A) & PAN/IO(H) are found to be twice than that of PAN/IO(B) composite nanofibers.

3.2. Adsorption Experiments

The PAN/IO(H), PAN/IO(B), and PAN/IO(A) composite nanofibers membrane were used as adsorbent for the adsorptive removal of CR dye from aqueous solution and their adsorption capacities have been compared. The effect of pH, contact time, initial concentration and temperature were also studied in the batch adsorption experiments.

3.2.1. Effect of pH

The pH of the solution is an important parameter that affects the whole adsorption process and particularly on the adsorption capacity, influencing not only the surface charge of the adsorbent, but also the solution dye chemistry.[19] It was observed that the dye solution changes its colour from red to dark blue when pH was adjusted in highly acidic range and highly basic range.[8] Therefore, to study the effect of pH for CR dye adsorption by the PAN/IO(H) nanofibers membrane, the initial pH of the dye solution was kept in the range of 3-10. The initial pH of CR dye solution was adjusted to the desired pH value using 0.1 M NaOH and 0.1 M HNO_3 solution. The graph of CR dye adsorbed with the variation of pH of the dye solution is shown in figure 7.

From figure 7 it was observed that the removal percentage of CR dye by the PAN/IO(H) nanocomposite fibers membrane increases with increasing pH, is maximum at pH 7 and at higher pH again it decreases. At lower pH, the hydroxyl groups present on the surface of the adsorbent were protonated. Simultaneously, the $–NH_2$- and $–SO_3^-$ groups of CR dye were also protonated to form $–NH_3^+$ and $–SO_3H$. Therefore, there was electrostatic repulsion between the positively charged surface of the adsorbent and the CR dye molecule resulting decrease in the adsorption quantity. At higher pH, there was competition between the hydroxyl ions and the negatively charged anionic dye molecule for the vacant adsorption sites of the adsorbent.[20] Still for higher and lower pH value, the removal percentage of dye molecule is over 70%. This suggested that physical adsorption may also have a contribution to the adsorption of dye due to the hydrogen bonding and inter-fibers porous structure of the nanofibers membrane. However, for neutral CR dye solution, the adsorption is maximum. This result could be attributed due to the fact that, hydrogen bonding, electrostatic interaction, complexation, coordination effect of metal atom with $–NH_2$- and $-SO_3^-$ groups are mainly

responsible for the adsorption of CR dye solution. Therefore, the pH of the CR dye solution was adjusted to 7 for the further adsorption studies. [21]

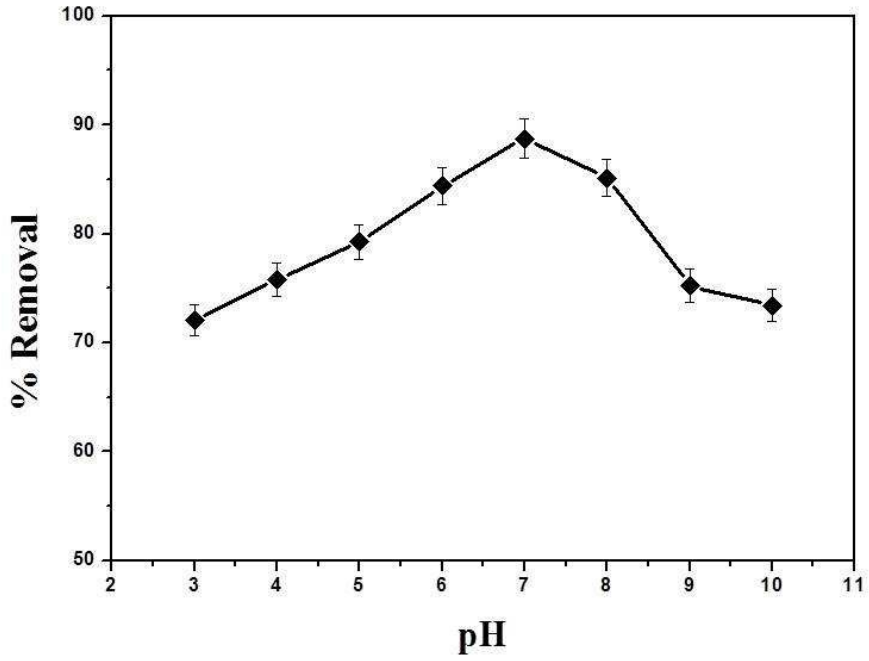

Figure 7: Removal percentage of CR dye by PAN/IO(H) composite nanofibers as a function of pH

3.2.2. Effect of Contact Time

It is very much essential to evaluate the effect of contact time required to reach equilibrium and to know the sorption kinetics for designing batch adsorption experiments. Therefore, the effect of contact time on the adsorption of CR dye onto the surface of PAN/IO nanocomposite fibers was investigated and the results obtained were shown in figure 8. From figure 8(a), it was observed that PAN/IO(H) composite nanofibers adsorbed 79% of the dye molecules within the first 15 minute of contact time. After 15 minute, the change in percentage adsorption became relatively slow and the equilibrium is achieved within 150 minute with 95% removal of CR dye molecules. The fast adsorption rate at the start of

contact time can be explained due to the fact that availability of the large number of active binding sites on the surface of the adsorbent during the initial stage. With a lapse of time, the adsorption capacity of the adsorbent became gradually exhausted since the few remaining vacant binding sites were difficult to be occupied due to the repulsive force between CR dye adsorbed on the surface of PAN/IO(H) nanocomposite fibers and present in solution phase.[22,23] In case of PAN/IO(A) composite nanofibers (figure 8(c)), it can be seen that 54% CR dye molecules adsorbed in the first 15 minute. The adsorption equilibrium is being achieved within 120 minute of contact time with a maximum dye removal of 92%. From figure 8(b), it was observed that in case of PAN/IO(B) composite nanofibers, the equilibrium is achieved within 120 minute of contact time with a 50% adsorption of dye molecules and the equilibrium adsorption capacity was found to be 10 mg/g. However, in case of PAN/IO(H) and PAN/IO(A) composite nanofibers, the equilibrium adsorption capacity was found to be 19 mg/g and 18.5 mg/g, respectively. These values are almost double than that of PAN/IO(B) nanocomposite fibers. The result can be explained due to the fact that, in case of PAN/IO(H) and PAN/IO(A) composite nanofibers, the iron oxide nanoparticles were grown on the surface of PAN nanofibers during hydrothermal reactions and the polymer nanofibers matrix not only acts as carrier of highly reactive iron oxide nanoparticles on its surface but also prevent the release of nanoparticles into water stream. This result is also further confirmed from EDAX studies. The weight percentage of iron in PAN/IO(H) and PAN/IO(A) composite nanofibers is observed to be two time higher than PAN/IO(B). Furthermore, in case of PAN/IO(B) nanocomposite fibers, the iron oxide nanoparticles are inside the PAN nanofibers matrix resulting lower adsorption capacity of CR dye molecule. We have also conducted the adsorption study of CR dye using un-functionalized electrospun PAN nanofibers and the percentage removal was observed to be 30% (figure not shown).

3.2.2.1. Kinetics Study

The study of adsorption kinetics describes the dye uptake rate at which it removed from aqueous solution and provides valuable data for understanding the mechanism of sorption reactions.[24,25] In our findings, two known kinetic models including pseudo-first-order equation and pseudo-second-order equation were applied to investigate the adsorption mechanism.

Firstly, pseudo-first-order equation has been widely used for analysing the adsorption of an adsorbate (CR dye) from aqueous solution. The differential equation for pseudo-first-order kinetic model is generally expressed as follows:

$$\frac{dq_t}{dt} = k_1(q_e - q_t) \quad (1)$$

Where k_1 is the rate constant of pseudo-first-order adsorption (min^{-1}), q_e is the equilibrium adsorption capacity (mg/g), and q_t is the amount of dye adsorbed at time t (mg/g). After definite integration, the above equation becomes:

$$ln(q_e - q_t) = lnq_e - k_1 \cdot t \quad (2)$$

The plot of $ln(q_e - q_t)$ versus t gives a straight line for the pseudo-first-order adsorption kinetics as shown in figure 8(d). The values of the pseudo-first-order rate constant k_1 and q_e can be obtained from the slope and intercept of the straight line (given in Table 1).

Secondly, the pseudo-second-order equation based on equilibrium adsorption is expressed as follows:

$$\frac{t}{q_t} = \frac{1}{k_2 \cdot q_e^2} + \frac{t}{q_e} \quad (3)$$

Where k_2 is the second-order-rate constant (g mg^{-1} min^{-1}), q_e is the equilibrium adsorption capacity (mg/g), and q_t is the amount of dye adsorbed at time t (mg/g). The linear plots of t/q_t

vs. t give the pseudo-second-order adsorption kinetics as represented in figure 8(e) and the values of k_2 and q_e can be determined from its slope and intercept (given in Table 1).

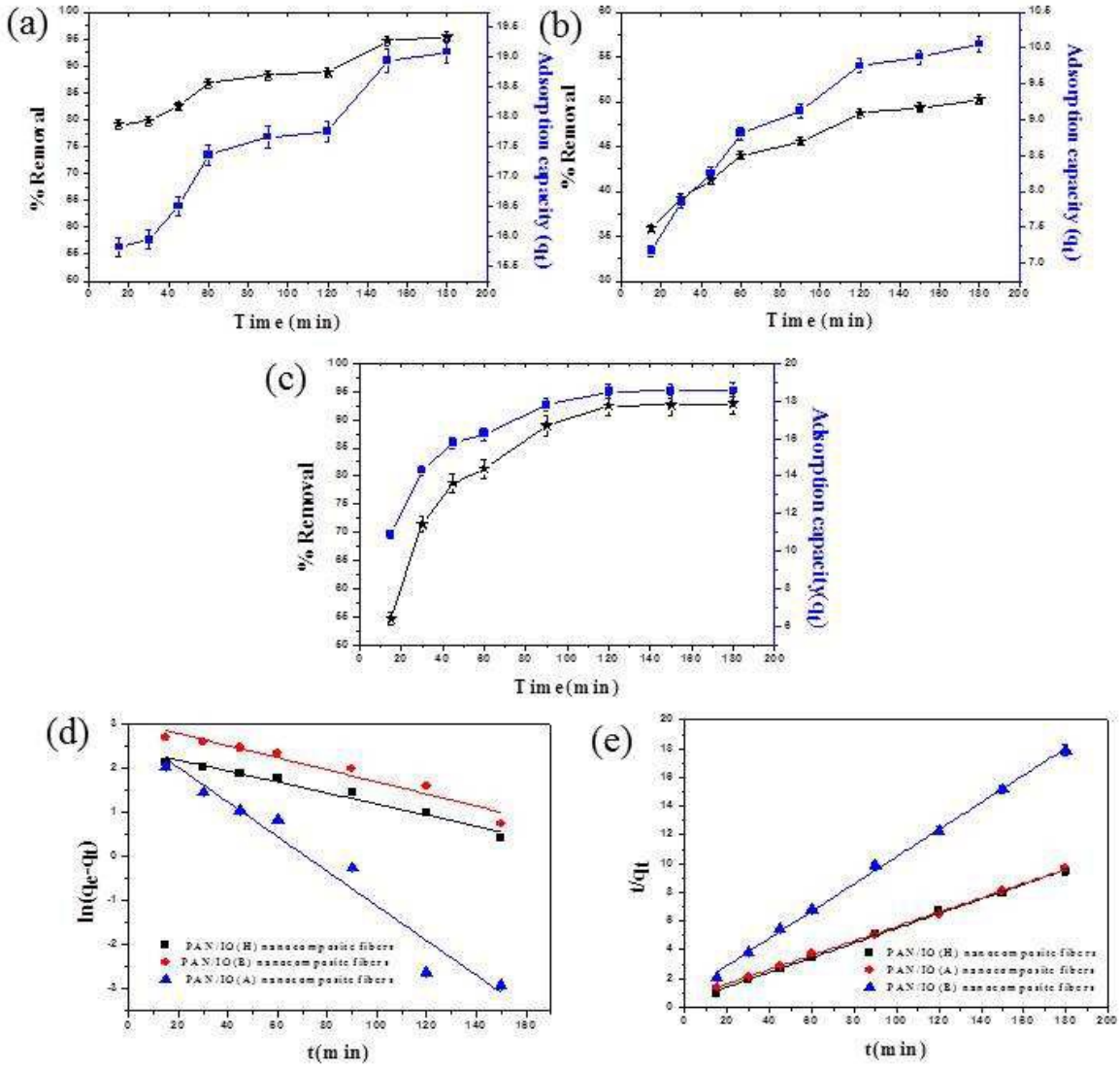

Figure 8: Effect of contact time on the adsorption of CR dye onto (a) PAN/IO(H), (b) PAN/IO(B) and PAN/IO(A) nanocomposite fibers, (c) Pseudo-first-order kinetic model and (d) Pseudo-second-order kinetic model for the adsorption of CR dye onto PAN/iron oxide nanocomposite fibers.

From figure 8(d), (e) and Table 1, it was observed that the values of linear correlation coefficient (R^2) for pseudo-first-order kinetic model are less than that of pseudo-second-order linear correlation coefficient. For pseudo-second-order equation, the calculated q_e values are extremely close to the experimental q_e value indicating that the kinetics data for adsorption of CR dye onto the PAN/iron oxide composite nanofibers is more in agreement to the pseudo-second-order kinetic model.

3.2.3. Effect of Initial Dye Concentration

The initial dye concentration is another important variable that can affect the adsorption process. In order to study the effect of initial dye concentration on the adsorption of CR dye onto the PAN/IO(H) composite nanofibers, the concentration of dye solution was varied from 20 to 70 mg/L, keeping the adsorbent dosage same (0.03 g) at three different temperature (303, 313 and 323 K). The results obtained were shown in figure 9. From figure 9(a), it was observed that the amount of dye adsorption increased from 12.8 to 40.7 mg/g with increasing initial concentration of CR dye from 20 to 70 mg/L at 303 K. This result can be explained due to the fact that, the initial dye concentration provides the driving force to overcome the resistance to the mass transfer of dye between the aqueous and the solid phase. At higher initial concentration, for a constant dosage of adsorbent, the availability of the adsorption sites of adsorbent becomes fewer and hence the removal of CR dye depends upon the initial dye concentration.[26] The increase in initial dye concentration also enhances the interaction between the adsorbent and the dye molecule. This result is also consistent with the result obtained by Dawood et al. (2012).[2]

3.2.3.1. Adsorption Isotherm Study

The equilibrium relationship between the quantity of adsorbate per unit of adsorbent (q_e) and its equilibrium concentration (C_e) at a constant temperature is known as the adsorption isotherm. Adsorption isotherms describe how pollutants interact with adsorbent materials and

so, are critical in optimizing the use of adsorbents. In order to optimize the design of an adsorption system to remove contaminants from solutions, it is important to establish the most appropriate correlation for the equilibrium curve.[27]Various isotherm models such as Langmuir, Freundlich and Dubinin-Radushkevich (D-R) isotherms models have been used to fit the adsorption data.

The Langmuir adsorption isotherm assumes that adsorption takes place at specific homogeneous sites within the adsorbent.[27] It is based on the physical hypothesis that the maximum adsorption capacity consists of a monolayer adsorption, that there is no lateral interaction between the adsorbed molecules and the adsorption energy is distributed homogeneously over the entire coverage surface.[28] The linear form of Langmuir isotherm equation can be written as:

$$\frac{C_e}{q_e} = \frac{C_e}{q_m} + \frac{1}{K_L \cdot q_m} \quad (4)$$

Where C_e is the equilibrium concentration of the adsorbate solution (mg/L), q_e is the equilibrium adsorption capacity (mg/g), q_m is the maximal adsorption capacity of the adsorbent (mg/g), and K_L is the Langmuir adsorption equilibrium constant (L/mg). The plot of C_e/q_e versus C_e gives the Langmuir adsorption isotherm as shown in figure 9(b). The values of q_m and K_L can be calculated from the slope and intercept of the plot and summarized in Table 2.

In contrast to Langmuir model, the Freundlich isotherm model is an empirical equation that describes the surface heterogeneity of the adsorbent. It considers the adsorption process as a multilayer one with a heterogeneous energetic distribution of active sites, accompanied by interactions between adsorbed molecules.[29] The linear form of Freundlich adsorption isotherm can be expressed as:

(5)

$$lnq_e = \frac{1}{n} \cdot lnC_e + lnK_F$$

Where q_e is the equilibrium adsorption capacity (mg/g), C_e is the equilibrium concentration of the adsorbate solution (mg/L); K_F (mg/g) and n are Freundlich constants related to the adsorption capacity and intensity of adsorption, respectively. The graphic of lnq_e versus ln C_e according to the Freundlich adsorption isotherm has been shown in figure 9(c). The values of Freundlich constants (K_F and n) can be calculated from the slope and intercept of the plot and listed in Table 2.

The Dubinin-Radushkevich isotherm model can also be used to describe adsorption on both homogenous and heterogeneous surfaces. Mathematically, this model can be expressed as:

$$q_e = q_m e^{-\beta \varepsilon^2} \quad (6)$$

A linear form of Dubinin-Radushkevich isotherm is

$$lnq_e = lnq_m - \beta \varepsilon^2 \quad (7)$$

Where q_m is the Dubinin-Radushkevich monolayer capacity (mg/g), β is a constant related to sorption energy (mg^2/J^2), and ε is the Polanyi potential, which is related to the equilibrium concentration as follows:

$$\varepsilon = RT\, ln\left(1 + \frac{1}{C_e}\right) \quad (8)$$

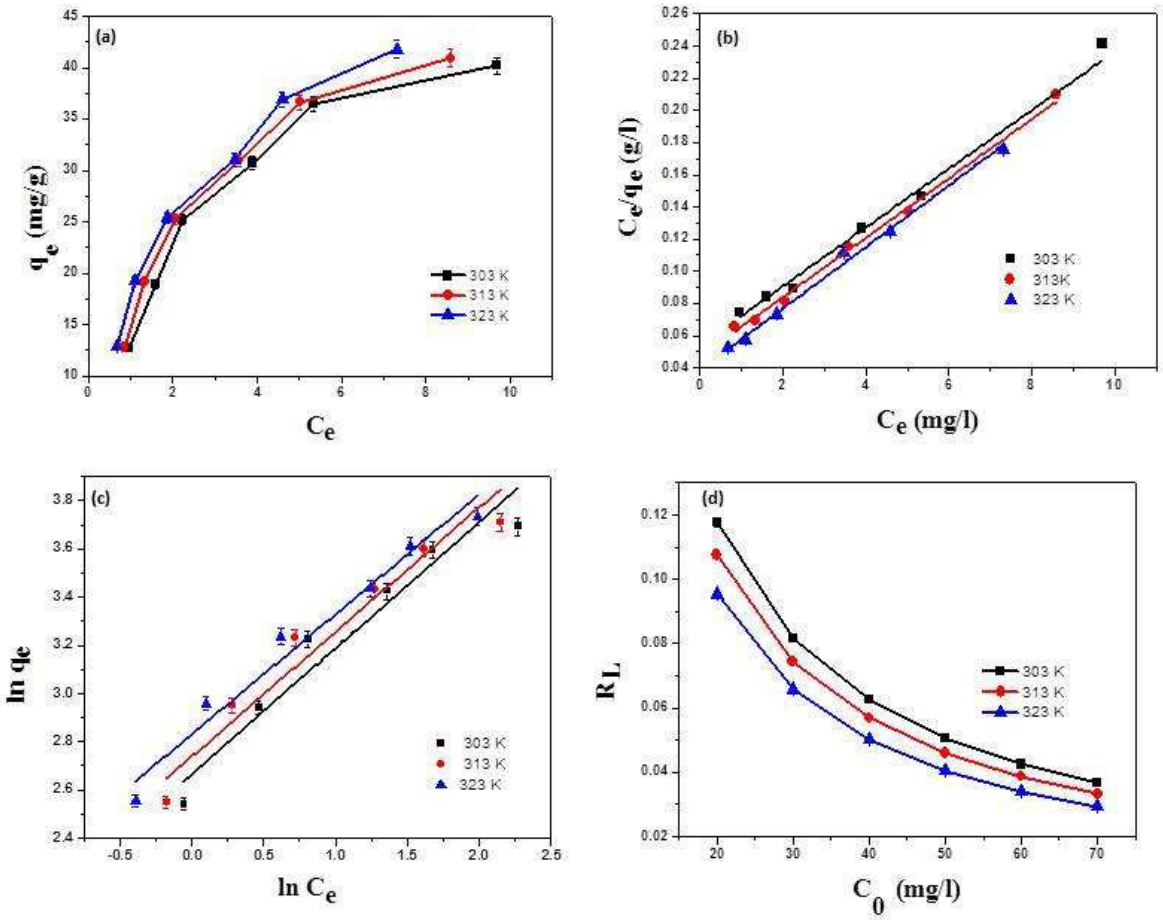

Figure 9: (a) Adsorption isotherms of CR dye onto the PAN/IO(H) nanocomposite fibers, (b) Langmuir adsorption isotherm, (c) Freundlich adsorption isotherm, and (d) R_L versus C_0 for adsorption of CR dye

Where R is the universal gas constant (8.314 J/molK) and T is the absolute temperature (K). The constant β gives the mean free energy (E) of adsorption per molecule of the adsorbate, when it is transferred to the surface of the solid from infinity in the solution and can be calculated using the relation:

$$E = \frac{1}{\sqrt{2\beta}} \qquad (9)$$

The magnitude of E is useful for estimating the mechanism of adsorption phenomenon. In the case of E < 8 kJ/mol, physical forces may affect the adsorption. If E is in the range of 8-16 kJ/mol, adsorption is governed by ion exchange mechanism, while for the values of E > 16 kJ/mol, adsorption may be dominated by particle diffusion mechanism.[30,31] The Dubinin-Radushkevich constants and correlation coefficients have been determined and presented in Table 2.

By comparing the values of the correlation coefficients (R^2) for these three different models we find that the Langmuir isotherm model yields the best fit (R^2 =0.9937). The correlation coefficients of Freundlich and Dubinin-Radushkevich adsorption isotherm models (R^2 =0.939, 0.9446) are relatively lower, so they are not suitable to describe the adsorption equilibrium process. Therefore the adsorption equilibrium of CR dye onto the PAN/IO(H) composite nanofibers can be best described with the Langmuir adsorption isotherm, which indicates the monolayer coverage and the homogeneous distribution of active sites on the nanofibers adsorbent. Similar result has also been reported for adsorption of CR dye onto the NiO/graphene nanosheets adsorbent.[32]

The essential feature of Langmuir adsorption isotherm can be expressed in terms of a dimensionless constant called separation factor (R_L),[27]which is defined by the following equation:

$$R_L = \frac{1}{1 + K_L C_0} \quad (10)$$

Where K_L is the Langmuir adsorption equilibrium constant (L/mg) and C_0 is the initial adsorbate concentration (mg/L). The R_L value is classified into different categories including R_L= 0, 0 < R_L < 1, and R_L > 1, suggesting that adsorption is irreversible, favourable, and unfavourable, respectively. The value of R_L varies in the range 0.029-0.11 (Table 2) confirms that the adsorption of CR dye onto the PAN/IO(H) composite nanofibers membrane is a

favourable process. The R_L value decreased with increasing initial concentration of the CR dye solution as shown in figure 9(d), which indicates that adsorption was more favourable at higher initial concentration of the CR dye solution.[33]

3.2.4. Thermodynamic Study

Thermodynamic parameters can provide additional in-depth information regarding the inherent energetic changes associated with the adsorption process.[34-35] The thermodynamic parameters, such as Gibbs free energy change (ΔG°), enthalpy change (ΔH°) and entropy change (ΔS°) can be calculated using the following thermodynamic equations:

$$K_c = \frac{C_s}{C_e} \tag{11}$$

$$\Delta G^0 = -RT\ ln(K_c) \tag{12}$$

The van't Hoff equation can be used to calculate the values of ΔH° and ΔS° as follows:

$$\ln(K_c) = -\frac{\Delta H^0}{RT} + \frac{\Delta S^0}{R} \tag{13}$$

Where K_c is the equilibrium constant of the adsorption, C_s is the amount of adsorbate adsorbed on adsorbent at equilibrium (mg/L) and C_e is the equilibrium concentration of the adsorbate in solution (mg/L). R is the universal gas constant (8.314 J/molK) and T is the absolute temperature (K). The plot of ln K_c versus 1/T (van't Hoff plot) resulted in a straight line is shown in figure 10.

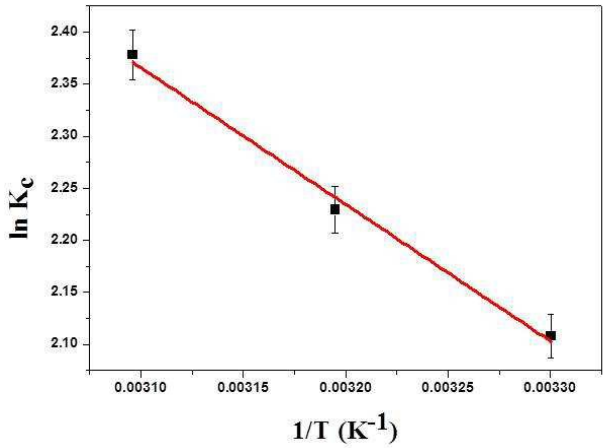

Figure 10: Van't Hoff plot for adsorption of CR dye onto the PAN/IO(H) composite nanofibers

As shown in figure 10, a linear fit (correlation coefficient, $R^2 = 0.9942$) was obtained for this adsorption process. The values of ΔH° and ΔS° are calculated from the slope and intercept of the straight line and the results obtained are given in Table 3. As presented in Table 3. As shown in Table 3, the values of ΔG° for adsorption of CR dye are -5.31, -5.8, and -6.38 kJ/mol at 303, 313 and 323 K, respectively. The ΔG° value is negative at all studied temperature, inferring that the adsorption of CR dye onto the PAN/IO(H) composite nanofibers would follow a spontaneous and favourable trend. The ΔG° value decreased with increase in temperature from 303 to 323 K, which revealed an increase in adsorption of CR dye with increasing temperature.[35] This result could be attributed due to the fact that increasing the mobility of the dye molecules and an increase in the number of active sites for the adsorption with increasing temperature.[2] The positive value of ΔH° (10.97 kJ/mol) confirms the endothermic nature of the adsorption event. The positive value of ΔS° (53.69 J/molK) shows the increased randomness at the solid-solution interface with some structural changes in the adsorbate and adsorbent and an affinity of the adsorbent towards the dye solution.[36]

3.2.5. Comparison study with previous results

Comparison of adsorption capacities of various adsorbents for the adsorptive removal of CR dye reported in literature and our prepared PAN/IO(H) composite nanofibers membrane are presented in Table 4. It is observed from the table that the maximum adsorption capacity (52.08 mg/g) of the prepared PAN/IO(H) composite nanofibers adsorbent is comparable to chitosan/montmorillonite nanocomposite and superior to other adsorbents reported. The results indicate number of adsorption sites per unit surface is higher for iron oxide immobilized PAN nanofibers compared to other materials studied. Hence the prepared

PAN/IO(H) composite nanofibers membrane is found to be an efficient adsorbent for the adsorptive removal of CR dye as well as other organic pollutants from waste water.

3.2.6. Mechanism for CR dye removal by PAN/IO composite nanofibers membrane

We have synthesized iron oxide functionalized PAN nanofibers by using three different methods as described earlier (figure 1). The formation and growth of iron oxide nanoparticles on the surface of PAN nanofibers in these two composite {PAN/IO(H) and PAN/IO(A)} nanofibers follows the proposed mechanism as shown in figure 11. The high adsorption capacities of PAN/IO(H) and PAN/IO(A) composite nanofibers adsorbent toward the removal of CR dye can be explained as follows. The point of zero charge (PZC) of iron oxide nanoparticles are reported to be 7.8-8.8 for the particle in the size range of 12-100 nm.[43] Therefore at the neutral pH (pH=7) the surface of the iron oxide nanoparticles are positively charged. So there is electrostatic attraction between the positively charged iron oxide nanoparticles and the negatively charged CR dye molecules. Hence the adsorption capacities of PAN/IO(H) and PAN/IO(A) composite nanofibers will enhance as compared to that of PAN/IO(B) and un-functionalized PAN nanofibers.

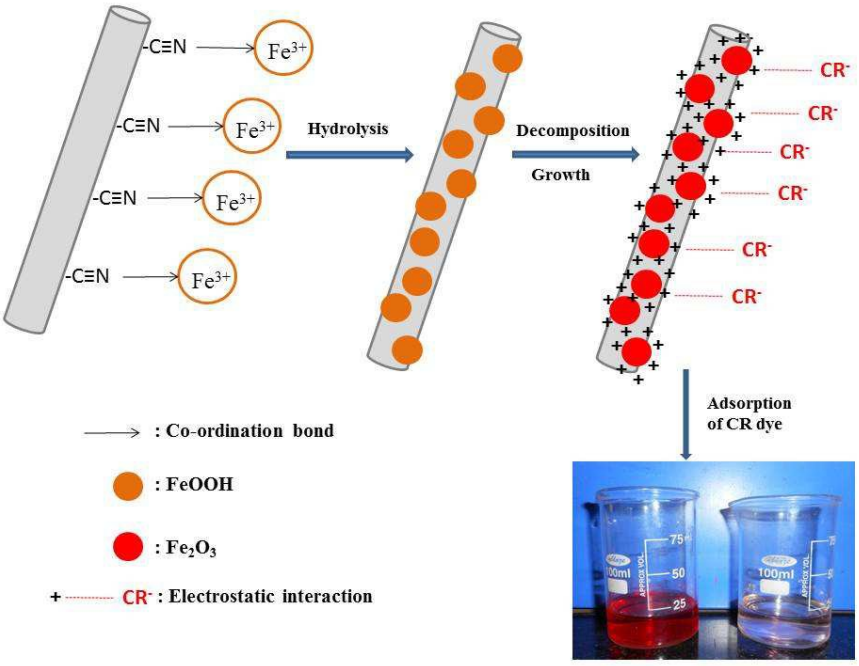

Figure 11: Schematic representation of iron oxide nanoparticles grown on the surface of PAN nanofibers and mechanism of CR dye removal

3.2.7. Leaching Test

In order to investigate the stability of PAN/IO(H) composite nanofibers with respect to metal leaching, the composite nanofibers membrane (0.03g) was kept in 20 mL of distilled water for 48 hours with constant stirring using a magnetic stirrer. Then the amount of Fe species coming off into the aqueous solution was analysed using ICP-AES. The amount of iron leached into the water was found to be very negligible (0.05 PPM) as revealed by ICP-AES. This study proves that iron oxide immobilized in PAN nanofibers membrane does not get leached significantly after 48 hours of stirring and hence can be used as efficient materials for sorption and membrane separation applications.

3.2.8. Desorption and reusability study

With rising prices of raw materials and waste water treatment processes, the stability and regeneration ability of the adsorbent during the adsorption process are important factors to its practical applications. Desorption studies can contribute to the elucidation of adsorption mechanism and recovery of the adsorbate and adsorbent.[2,32] The main objective of the regeneration process is to restore the adsorption capacity of exhausted adsorbent and to recover valuable components present in the adsorbed phase. Desorption study was carried out by taking 0.03 g of CR loaded PAN/IO(H) composite nanofibers membrane in 20 mL of 0.01mol/L NaOH solution for 3 h. Then the concentration of eluted CR was measured to calculate the amount of CR desorbed in the solution. In order to study the regeneration of the adsorbent, successive adsorption-desorption processes were carried out for four consecutive cycles which is shown in figure S1 (supplementary data). The figure shows that about 95 and 86% of CR dye could be effectively adsorbed in the first cycle and the second cycle, respectively. After that the adsorption capacity of the composite nanofibers adsorbent

decreases as the number of cycle increases. However, the adsorption capacity of the PAN/IO(H) nanofibers adsorbent still remained 70% at the end of the fourth cycle.

4. Conclusions

We have successfully synthesized PAN nanofibers functionalized with iron oxide nanoparticles by three different methods to obtain PAN/IO(H), PAN/IO(A) and PAN/IO(B) composite nanofibers membrane. The prepared PAN/iron oxide composite nanofibers were used as adsorbent for the adsorption of CR dye from aqueous solution. It was observed that the equilibrium adsorption capacities of in-situ iron oxide immobilized PAN {PAN/IO(H) and PAN/IO(A)} composite nanofibers were found to be twice than that iron oxide nanoparticles blended PAN {PAN/IO(B)} nanofibers. The adsorption of CR dye onto the PAN/IO(H) nanocomposite fibers fitted well with the Langmuir adsorption isotherm with maximum adsorption capacity of 52.08 mg/g and follows pseudo-second-order kinetic model with rate constant of 0.007 g/mg min. The thermodynamic result indicates that the adsorption process was spontaneous and endothermic in nature over the temperature range of 30° to 50°C. The leaching study confirms that there is no significant leaching of iron species into water media. The present work suggests that iron oxide incorporated PAN composite nanofibers have a great potential as next generation nanoadsorbents for the removal of CR dye owing to their simple preparation, high sorption capacity and low cost.

Acknowledgement

The authors would like to acknowledge NIT, Rourkela for funding and providing the research facility.

References

1. M. C. S. Reddy, L. Sivaramakrishna and A. V. Reddy, *J. Hazard. Mater*., 2012, **203-204**, 118.
2. S. Dawood and K. Sen, *Water Res*., 2012, **46**, 1933.
3. A. Afkhami and R. Moosavi, *J. Hazard. Mater*., 2011, **174**, 398.
4. O. Turgay, G. Ersoz, S. Atalay, J. Fross and U. Welander, *Sep. Purif. Technol*., 2011, **79**, 26.
5. A. Criscuoli, J. Zhong, A. Figoli, M. C. Carnevale, R. Huang and E. Drioli, *Water. Res*., 2008, **42**, 5031.
6. K. Pazdzior, A. Klepacz-Smolka, S. Ledakowicz, J. Sozka- Ledakowicz, Z. Mrozinska and R. Zylla, *Chemosphere*, 2009, **75**, 250.
7. S. Wang and E. Ariyanto, *J. Colloid. Interface. Sci*., 2007, **314**, 25.
8. A. Mahapatra, B. G. Mishra and G. Hota, *Ceram. Int*. 2013, **39**, 5443.
9. G. R. Xu, J. N. Wang and C. J. Li, *Chem. Eng. J*., 2012, **198-199**, 310.
10. C. J. Li, Y. J. Li, J. N. Wang and J. Cheng, *Chem. Eng. J*. 2013, **220**, 294.
11. H. J. Kim, H. R. Pant, C. H. Park, L. D. Tijing, N. J. Choi and C. S. Kim, *Ceram. Int*., 2013, **39**, 3095.
12. F. Pan, Q. Cheng, H. Jia and Z. Jiang, *J. Membr. Sci*., 2010, **357**, 171.
13. J. Zhu, S. Wei, X. Chen, A. B. Karki, D. Rutman, D. P. Young and Z. Guo, *J. Phys. Chem*., 2010, **114**, 8844.
14. H. Zhang, H. Nie, D. Yu, C. Wu, Y. Zhang, C. J. B. White and L. Zhu, *Desalination*, 2010, **256**, 141.
15. R. Nirmala, K. Jeon, R. Navamathavan, B. S. Kim and M. S. Khil, *J. Collloid. Interface. Sci*., 2013, **397**, 65.
16. M. Khosravi and S. Azizian, *J. Ind. Emg. Chem*., 2014, **20**, 2561.
17. N. Tian, X. Tian, L. Ma, C. Yang, Y. Wang, Z. Wang and L. Zhang, *RSC advances*, 2015, **5**, 25236.
18. B. Junga, J. K. Yoon, B. Kima and H. W. Rhee, *J. Membr. Sci*., 2005, **246**, 67.
19. R. Zhang, J. Zhang, X. Zhang, C. Dou and R. Han, *J. Taiwan. Inst. Chem. Eng*., 2014, **45**, 2578.
20. L. Li, X. Li, H. Duan, X. Wang and C. Luo, *Dalton Trans*., 2014, **43**, 8431.
21. R. Kumar, J. Rashid and M. A. Barakat, *RSC Advances*, 2014, **4**, 38338.
22. W. C. Wanyonyi, J. M. Onyari and P. M. Shiundu, *Energy Procedia*, 2014, **50**, 862.
23. S. Kour, S. Rani, V. Kumar, R. K. Mahajan, M. Asif, I. Tyagi and V. K. Gupta*, J. ind. Eng. Chem*., 2014, http://dx.doi.org/10.1016/j.jiec.2014.11.035
24. R. Sharma, N. Singh, S. Tiwari, S. K. Tiwari, S. R. Dhakate, *RSC Adv*., 2015, **5**, 16622.
25. X. Li, R. Zhao, B. Sun, X. Lu, C. Zhang, Z. Wang and C. Wang, *RSC Adv*., 2014, **4**, 42376.
26. Z. Shahryari, A. S. Goharrizi and M. Azadi, *Int. j. Water Res. Environ. Eng.*, 2010, **2**, 16.
27. M. Iram, C. Guo, Y. Guan, A. Ishfaq and H. Liu, *J. hazard. Mater.*, 2010, **181**, 1039.
28. A. Afkhami and R. Moosavi, 2010, **174**, 398.
29. R. Liu, H. Fu, H. Yin, p. Wang, L. Lu and Y. Tao, *Powder Technol*., 2015, **274**, 418.
30. E. Bulut, M. Ozakar and I. A. Sengil, *Microporous Mesoporous Mater.,* 2008, **115**, 234.
31. S. Sharma and K. Balasubramanian, *RSC Adv*., 2015, **5**, 31732.
32. X. Rong, F. Qiu, J. Qin, H. Zhao, J. Yan and D. Yang, *J. Ind. Eng. Chem*., http://dx.doi.org/10.1016/j.jiec.2014.12.009.
33. X. Li, C. Zhang, R. Zhao, X. Lu, X. Xu, X. Jia, C. Wang, and L. Li, *Chem. Eng. J*., 2013, **229**, 420.

34. S. Zeng, S. Duan, R.Tang, L. Li, C. Liu and D. Sun, *Chem. Eng. J*., 2014, **258**, 218.
35. J. Wang, K. Pan, E. P. Giannelis and B. Cao, *RSC Adv*., 2013, **3**, 8978.
36. S. Wang, W. Boyjoo, A. Choueib and Z. H. Zhu, *Water Res*., 2005, **39**, 129.
37. B. Cheng, Y. Le, W. Cai and J. Yu, *J. hazard. Mater*.,, 2011, **185**, 889.
38. M. Ghaedi, H. Tavallali, M. Sharifi, S. N. Kokhdan and A. Asghari, *Spectrohimica Acta Part A*, 2012, **86**, 107.
39. L. Wang and A. Wang, *J. hazard. Mater.*, 2007, **147**, 979.
40. M. Arslan and M. Yigitoglu, J. Appl. Polym. Sci., 2008, **107**, 2846.
41. C. Yu, X. Dong, L. Guo, J. Li, F. Qin, L. Zhang, J. Shi and D.Yan, J. Phys. Chem. C, 2008, **112**, 13378.
42. S. Nouri, F. Haghseresht and G. Q. M. Lu, *Adsorption*, 2002, **8**, 215.
43. E. M. Hotze, T. Phenrat, G. V. Lowry, *J. Environ. Qual*., 2010, **39**, 1909

Table 1: Kinetic parameters for adsorption of CR dye onto the PAN/Iron oxide nanocomposite fibers

	$q_{e,exp}$ (mg/g)	Pseudo-first order			Pseudo-second order		
		$k_1(min^{-1})$	$q_{e,cal}$ (mg/g)	R^2	k_2 (g mg^{-1} min^{-1})	$q_{e,cal}$ (mg/g)	R^2
PAN/IO(H)	19.09	0.012	11.51	0.963	7.14×10^{-3}	19.57	0.9972
PAN/IO(A)	18.57	0.039	16.44	0.949	4.1×10^{-3}	20.09	0.9993
PAN/IO(B)	10.05	0.013	21.6	0.9304	8.9×10^{-3}	10.5	0.9983

Table 2: Langmuir, Freundlich and Dubinin-Radushkevich isotherm constants for adsorption of CR dye onto the PAN/IO(H) nanocomposite fibers

	Langmuir				Freundlich			Dubinin-Radushkevich			
Temperature (K)	q_m (mg/g)	K_L (L/mg)	R^2	R_L	K_F (mg/g)	n	R^2	q_m (mg/g)	β (mg^2/J^2)	E (kJ/mol)	R^2
303	52.08	0.37	0.9937	0.11-0.036	14.83	2.01	0.939	36.41	3×10^{-7}	1.291	0.9446
313	52.91	0.41	0.9967	0.1-0.033	15.89	2.03	0.95	37.01	3×10^{-7}	1.29	0.9563
323	53.19	0.47	0.9943	0.09-0.029	17.24	2.08	0.97	36.99	2×10^{-7}	1.581	0.9388

Table 3: Thermodynamic parameters for adsorption of CR dye onto the PAN/IO(H) nanocomposite fibers

T (K)	K_c	ΔG° (kJ/mol)	ΔH° (kJ/mol)	ΔS° (J/molK)
303	8.23	–5.31	+10.97	+53.69
313	9.29	–5.8		
323	10.78	–6.38		

Table 4: Comparison of adsorption capacities of various adsorbents for removal of CR dye

Adsorbent	q_m (mg/g)	Isotherm model	References
Reagent NiO nanoparticles	39.70	Langmuir	[37]
Activated carbon from Myrtus communis (AC-MC)	19.231	Langmuir	[38]
Chitosan/montmorillonite nanocomposite	54.52	Langmuir	[39]
4-Vinyl pyridine grafted poly(ethylene terephthalate fibers	18.1	Langmuir	[40]
Mesoporous Fe_2O_3	53		[41]
Acid activated red mud	7.08		[42]
Acid treated pine cone	40.19	Langmuir	[2]
PAN/IO(H) nanocomposite fibers	52.08	Langmuir	present study

Table of Contents (TOC)

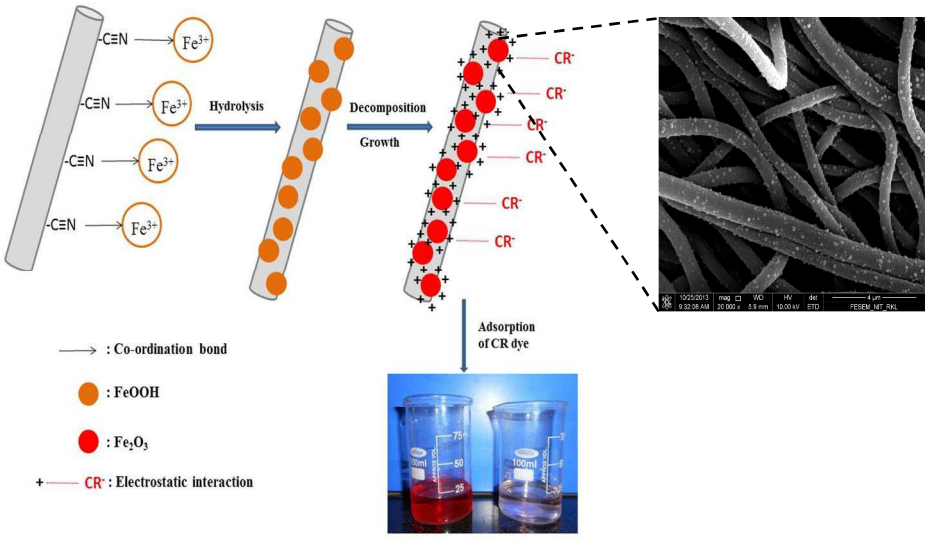

Iron oxide nanoparticles grown on the surface of electrospun PAN nanofibers membrane can be used as a next generation nanoadsorbent for effective removal of CR dye